Received December 15, 2020, accepted January 3, 2021, date of publication January 14, 2021, date of current version January 22, 2021.

*Digital Object Identifier 10.1109/ACCESS.2021.3051760*

# ATOMIC: Adaptive Transmission Power and Message Interval Control for C-V2X Mode 4

**BYUNGJUN KANG[1], JINMO YANG[2], JEONGYEUP PAEK[3], (Senior Member, IEEE), AND SAEWOONG BAHK[2], (Senior Member, IEEE)**

[1]Samsung Research, Samsung Electronics Company, Ltd., Suwon-si, South Korea
[2]Department of Electrical and Computer Engineering, INMC, Seoul National University, Seoul 08826, South Korea
[3]School of Computer Science and Engineering, Chung-Ang University, Seoul 06974, Republic of Korea

Corresponding author: Saewoong Bahk (sbahk@netlab.snu.ac.kr)

This work was supported by the Institute of Information and communications Technology Planning and Evaluation (IITP) grant funded by the Korean Government (MSIT) (Scalable Spectrum Sharing for Beyond 5G Communication) under Grant 2018-0-00923.

**ABSTRACT** To support the emerging vehicle-to-everything (V2X) communication for autonomous vehicles and smart transportation services, 3rd Generation Partnership Project (3GPP) has recently introduced cellular V2X (C-V2X) standards. In C-V2X, radio resources can be managed not only centrally by the cellular network base station, but also in a completely distributed manner (*Mode 4*) without any cellular support. However, *Mode 4* may suffer significant collisions and interference in a dense environment since each vehicle selects its own resources to transmit V2X messages autonomously without adapting appropriately to vehicle density. To address this challenge, we propose *ATOMIC*, an *Adaptive Transmission pOwer and Message Interval Control scheme for C-V2X Mode 4*, in which each vehicle utilizes real-time channel sensing and neighbor information to reduce channel contention for improved reliability and latency. Through analysis and extensive simulations, we show that *ATOMIC* outperforms the standard *Mode 4* in both urban and highway scenarios especially in highly dense environments.

**INDEX TERMS** Vehicle-to-vehicle (V2V) communication, vehicle-to-everything (V2X), cellular V2X (C-V2X) mode 4, TX power adaptation, rate control.

## I. INTRODUCTION

Wireless communication technology will play a key role in the emerging vehicular networks as the demand for cooperative and autonomous driving increases. For this purpose, IEEE 802.11p-based wireless technologies such as the dedicated short range communication (DSRC) [2]–[4] or wireless access in vehicular environments (WAVE) [5]–[7] have been widely studied for vehicular communication [8], [9]. In addition, as an alternative to IEEE 802.11p, 3GPP introduced cellular vehicle-to-everything (C-V2X) standards in Release 14 to support vehicle-to-vehicle (V2V), vehicle-to-infrastructure (V2I), and vehicle-to-pedestrian (V2P) services using LTE technology [10]. While C-V2X uses legacy Uu interface (uplink and downlink) defined between vehicles and base stations for V2I communication, it also supports V2V direct communication over *sidelink* defined between vehicles. The use of cellular network capable of supporting mobile velocity of around 350 km/h made low end-to-end latency possible [11]. The fact that the network has already been deployed is another main advantage of LTE.

Recently, C-V2X has evolved towards fifth-generation new radio (5G NR) V2X in Release 16 [12]–[15]. Release 16 builds on Release 14 by introducing a NR-based sidelink with added flexibility in subcarrier spacing and sensing periods, and supports unicast and multicast transmissions in addition to broadcast transmissions. However, there are many parameters to be determined in resource selection procedure in section 8.1.4 such as $(t_0^{SL}, t_1^{SL}, t_2^{SL}, \ldots)$, which is the set of slots which can belong to a sidelink resource pool, $T_{proc,1}$ [14]. Since the specification for NR V2X is not completed and the procedure of C-V2X in Release 14 is not quite different from that of NR V2X in Release 16 except for some minor changes such as flexible sensing periods, we consider C-V2X for Release 14 in this work and it can be applied to NR V2X in future work.

The associate editor coordinating the review of this manuscript and approving it for publication was Mostafa Zaman Chowdhury.

C-V2X supports two modes of operation for resource scheduling, *Mode 3* and *Mode 4*. In Mode 3, UEs make transmission requests to a base station which then allocates resources, similar to legacy scheduling in cellular networks. This centralized allocation has the advantage of having a better view of the network. However, there are two major limitations; (1) UEs should stay connected to get scheduled, and this incurs significant signaling overhead especially during handover for highly mobile devices. Furthermore, (2) Mode 3 is unable to manage resource allocation for out-of-coverage vehicles; i.e., V2V transmissions are completely blocked when vehicles lose network coverage even if they are in direct communication range of each other. These limitations of Mode 3 led to the design of Mode 4 where each UE selects its own transmission resources in a decentralized manner without any cellular support. UE's autonomous scheduling allows V2V communication to operate irrespective of network coverage, and for this reason, Mode 4 is often considered as the baseline mode for C-V2X [16], [17].

One of the key components in C-V2X system is the *cooperative awareness message* (CAM) [18] which a vehicle periodically broadcasts to inform its updated status including identification, state, velocity and location to its neighboring vehicles, as well as public safety information such as accident events. *Awareness distance* is defined as the maximum range that a CAM can be received, and all vehicles within this distance from the source vehicle are regarded as neighbors. Exchange of CAMs allow every vehicle to obtain an accurate and newest awareness of the dynamics of surrounding vehicles [19].

Reliable and robust delivery of CAMs would be crucial for such purposes. However, this is challenging for Mode 4 due to lack of centralized information, especially in a highly dynamic wireless environment with mobile vehicles. Specifically, Mode 4 may suffer from significant collisions and interference in a dense environment since each vehicle selects its own resources to transmit V2X messages without adapting appropriately to vehicle density. We show this problem through C-V2X simulator in Section IV.

To address the problem, this work tackles the *sensing-based semi-persistent scheduling* (SPS) algorithm in Mode 4 to propose *ATOMIC*, an *Adaptive Transmission pOwer and Message Interval Control scheme for C-V2X Mode 4*. *ATOMIC* is an enhancement to SPS in which each vehicle exploits real-time channel sensing and neighbor information to reduce channel contention for improved reliability and latency. Specifically, we design a message interval control algorithm by analyzing the collision probability according to CAM transmission rate, and also design a transmission power adaptation algorithm by analyzing the optimal transmission power which has the highest expected packet reception ratio (PRR) given the awareness of the surrounding neighborhood. Then, these two are combined so that each UE can adaptively find an appropriate set of parameters for reliable CAM delivery depending on the channel state and density of the network.

We evaluate *ATOMIC* through extensive simulations in various scenarios where the communication network behavior from the lower physical layer to the medium access and congestion control, including issues of hidden terminal phenomena and capture effects, are taken into account.

The contributions of this work are threefold:

- We first show that the performance of C-V2X Mode 4 is degraded significantly in high-density environments due to saturation of wireless medium and resource collisions.
- We propose *ATOMIC*, a standard-compliant algorithm that adapts to the density of neighboring vehicles and measured sidelink signal strength.
- We demonstrate through extensive simulations that *ATOMIC* outperforms the standard C-V2X Mode 4 in both highway and urban scenarios built on actual road maps.

The remainder of this article is organized as follows. Section II presents a brief overview of C-V2X Mode 4, and Section III summarizes related work in the literature. Then, Section IV motivates our work by discussing the problem of C-V2X Mode 4 in dense environments and the impact of transmission power and message interval on system performance. Based on these observations, Section V describes the design of *ATOMIC*. Section VI evaluates the proposed algorithm, Section VII concludes our work.

## II. BACKGROUND

This section provides a brief overview of C-V2X Mode 4 as well as the requirements for safety applications defined by standardization entities.

### A. C-V2X Mode 4

C-V2X supports 10 and 20 MHz bandwidth on 5.9 GHz Intelligent Transportation System (ITS) band for vehicular sidelink communication. It uses *single carrier frequency division multiple access* (SC-FDMA), and thus each channel is divided into several time-frequency resource pairs. Each pair has a minimum unit of one subframe (1 ms) in time, and one *sub-channel* in frequency. A sub-channel is a group of *resource blocks* (RBs, 180 kHz), where an RB is the smallest unit of frequency resources in LTE. The number of RBs per sub-channel can vary depending on the size of the transmission and the modulation and coding scheme (MCS) level used for that transmission. Sub-channels can be used to transmit both the data including V2X messages, and also the associated control messages known as the *sidelink control information* (SCI). SCI carries the scheduling information for data transmissions, and Mode 4 uses SCI format 1 (shown later in Section V).

In C-V2X Mode 4, each vehicle independently selects an appropriate (hopefully unused and clear) set of transmission resources based on the channel sensing results, and reserves them for future transmissions. This scheme is referred to as the *sensing-based semi-persistent scheduling* (SPS), and Figure 1 illustrates an example operation. A group of RBs

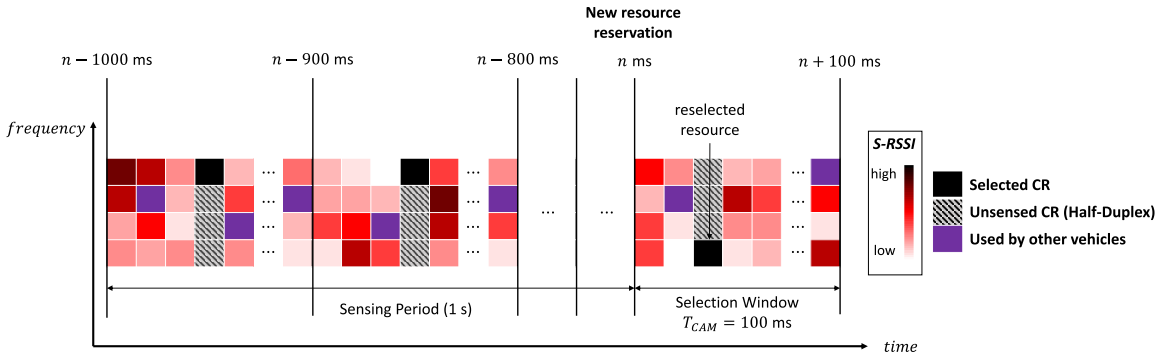


**FIGURE 1.** Sensing-based SPS for C-V2X Mode 4.

for transmitting a CAM packet is hereafter denoted as CAM resource (CR), which is the unit of resource selection in C-V2X Mode 4. The concept of CR is similar to Resource Block Group (RBG) in 3GPP standard [12], which is bundled by multiple number of consecutive RBs and is used for the unit of resource allocation. Specifically, each vehicle executes the following steps for V2X message transmissions.

*Stage 1 - Channel Sensing:* A vehicle continuously measures the *sidelink received signal strength indication* (S-RSSI) on each sub-channel every subframe as a measure of interference, and collects the sensing measurements for a pre-defined sensing period, typically set to 1 second.

*Stage 2 - Available Resource List:* Based on the channel sensing measurements, the vehicle creates its own candidate resource list, $RL_A$, which contains all available radio resources excluding those that fall under the following conditions:

- S-RSSI of the RB is higher than a certain threshold, and
- the RB will be occupied (reserved) by other vehicles, which is identified in the SCI from those vehicles.

If the size of $RL_A$ ($|RL_A|$) is smaller than 20% of the number of all RBs in a CAM interval, Stage 2 is executed iteratively with 3 dB-increased threshold until $|RL_A|$ becomes larger than 20%. Otherwise, the vehicle continues to execute the following stages.

*Stage 3 - Resource selection:* The vehicle identifies the best 20% resources, $RL_C$ (i.e., the RBs having the lowest 20% S-RSSI values), among $RL_A$. Finally, the vehicle randomly selects a group of RBs (a CR) among $RL_C$ of which the number is determined by the size of CAM and MCS level, and reserves the same frequency resources for a random number of subsequent CAM transmissions with the same transmission interval. The number of subsequent CAM message transmissions reserved can lie between 5 and 15 for transmitting CAM with periodicity of 10 Hz. Since the SPS also supports transmitting CAM with periodicity of 20 and 50 Hz, the number of subsequent CAM transmissions is randomly selected between 10 and 30 for 20 Hz, and between 25 and 75 for 50 Hz, respectively. We focus on 10 Hz transmission in this work which is default in C-V2X Mode 4.

*Stage 4 - Resource re-selection:* After each packet transmission, the number of remaining consecutive reservation denoted as *SPS counter* decreases. When the SPS counter reaches zero, the vehicle decides to maintain the same resources with probability $p_k$ or reselect the resources with probability $(1 - p_k)$.

### B. SAFETY REQUIREMENTS

There are four well-known organizations that work on standardizing vehicular communication: 3GPP and European Telecommunications Standards Institute (ETSI) in Europe, National Highway Traffic Safety Administration (NHTSA) in U.S., and the Society of Automotive Engineers (SAE). They announce and describe various safety and non-safety scenarios, and list their requirements (e.g. message periodicity) for each scenario [20]–[22]. Those are summarized in TABLE 1. Each safety application may have different range requirements, and the communication range specified by NHTSA (only) has values from 150 to 500 m. As the name of NHTSA implies, these ranges are only applicable to highway scenarios, and are not suitable for dense urban scenarios [23]. Based on these requirements, we adopt different communication ranges for different scenarios in this work.

## III. RELATED WORK

Several prior work have studied the performance of SPS algorithm for C-V2X Mode 4. Molina-Masegosa and Gozalvez compared Mode 4 with a random resource allocation scheme in terms of PRR in a Manhattan grid [24] and a highway scenario [25]. Furthermore, Wang *et al.* [26] and Nguyen *et al.* [27] compared the average PRRs of C-V2X Mode 4 and IEEE 802.11p according to transmitter-receiver distance. Bazzi *et al.* investigated the impact of PHY and MAC parameters on PRR in C-V2X Mode 4 [28].

While aforementioned prior work studied the performance of C-V2X Mode 4 as is, a few studies have also discussed its problems and considered enhancements. For example, C-V2X Mode 4 selects its resources by calculating the linear

**TABLE 1. Safety applications and requirements.**

| Safety application (suggested by organizations) | Periodicity (Hz) | Range (m) |
|---|---|---|
| **3GPP** | | |
| Forward collision warning | 10 | N/A |
| V2V emergency stop use case | 10 | N/A |
| V2I emergency stop use case | 10 | N/A |
| Queue warning | N/A | N/A |
| Vulnerable road user safety | 1 | N/A |
| **ETSI** | | |
| Emergency vehicle warning | 10 | N/A |
| Motorcycle warning | 2 | N/A |
| Vulnerable road user warning | 1 | N/A |
| Lane change assistance | 10 | N/A |
| Cooperative glare reduction | 2 | N/A |
| Cooperative forward collision warning | 10 | N/A |
| **NHTSA** | | |
| Wrong way driver warning | 10 | 500 |
| Cooperative forward collision warning | 10 | 150 |
| Lane change warning | 10 | 150 |
| Highway merge assistant | 10 | 250 |
| Highway/rail collision warning | 1 | 300 |
| Cooperative glare reduction | 1 | 400 |

average of S-RSSI on each of the resource blocks during a sensing window. However, physical channel of highly dynamic vehicular environment may fluctuate rapidly over time. To deal with this, Abanto-Leon *et al.*proposed a non-linear power averaging with exponential weighting where recent S-RSSI measurements are assigned higher priority [29].

A few prior work investigated the feasibility of implementing the distributed congestion control (DCC) algorithm specified in SAE J2945/1 standard [30], which is based on IEEE 802.11p, on the top of the C-V2X stack. Among various techniques suggested in the standard to mitigate congestion, Mansouri *et al.* [31] employed only transmission rate control, which changes the frequency of CAM according to the measured density of vehicles. However, the authors only show the feasibility of DCC algorithm on C-V2X without any specific scheme for the rate adaptation. On the other hand, Toghi *et al.* [32] considered transmission 'range' control using power adaptation in addition to transmission rate control. Since DCC algorithm proposed in the standard is designed for DSRC communication, they modified the algorithm to operate in C-V2X networks. However, their transmission rate control algorithm with 1 ms granularity is not backward compatible with the standard as mentioned in Section V.

Kang *et al.* investigated the impact of transmit power in C-V2X, and proposed a simple power control algorithm which allocates transmission power inversely proportional to the sum of S-RSSI values in the same subframe with newly re-selected resource [1], [33]. Their approach is to use the sum of S-RSSI values to infer the total amount of potential interference, and reduce the network-wide interference level by decreasing the transmit power of a vehicle. However, the sum of S-RSSI values in the same subframe without considering in-band emission factor, which is the average energy level leaked from adjacent subchannels, is not an exact amount of potential interference. Furthermore, their algorithm may converge to an unfair state because, if a few vehicles start with high transmit power, other vehicles will sense high S-RSSI sum and use low transmit power, and this state will remain until high-power vehicles dissappear.

**TABLE 2. System parameters for Mode 4.**

| Parameter | Constraints | Used |
|---|---|---|
| Sensing period (s) | 1 | 1 |
| Threshold of the power level (dBm) | [-128, -2] | -110 |
| First subframe for a new allocation ($T_1$) | [1, 4] | 1 |
| Last subframe for a new allocation ($T_2$) | [20, 100] | 100 |
| Probability to keep the resource ($p_k$) | [0, 0.8] | 0 |

**TABLE 3. Simulation settings.**

| Parameter | Highway | Manhattan |
|---|---|---|
| Map size | 4 km (3+3 lanes) | 22 km$^2$ |
| Awareness distance | 150 m | 80 m |
| CAM size | 300 bytes | |
| Bandwidth | 10 MHz | |
| Antenna gain | 3 dB | |
| Propagation model | WINNER+, Scenario B1 | |
| Shadowing variance | 3 dB (LOS), 4 dB (LNOS) | |
| Minimum SINR ($\eta$) | 2.76 dB (MCS 4), 7.30 dB (MCS 7) | |

## IV. PROBLEM AND MOTIVATION

Our work is motivated by observing the impact of vehicle density, transmission power, and message interval on CAM reception performance.

For this purpose, we use two different transmission power settings, 23 dBm and 10 dBm. Our choice of the two settings is justified as follows. Currently, 23 dBm is the maximum transmission power defined in the 3GPP standard for sidelink communication of normal vehicle UEs [16], and it is typically used in the literature for evaluations [28], [34]–[37]. 10 dBm is chosen from the Car-to-Car Communication Consortium (C2C-CC) requirement on ITS stations [38] stating that, upon detecting signal from a tolling system such as CEN-DSRC [39], [40], vehicle UEs should immediately reduce transmission power of the sidelink to pDccPToll, whose value is 10 dBm, to avoid excessive interference to the tolling system. This procedure is based on the detect-and-avoid method specified in [41]. Note that transmission power is directly related to 'effective density' since longer transmission range means more vehicles in awareness distance.

We simulate C-V2X Mode 4 using the LTEV2Vsim simulator [42] which is a system-level simulator designed for investigation of resource allocation algorithms in C-V2X. It implements the 3GPP Release 14 standard for sidelink communication. All vehicles transmit CAMs of 300 bytes at periodicity of 10 Hz, and MCS level is 4. As recommended by 3GPP in [43], we use the WINNER+ model, scenario B1, for the propagation model. Mode 4 parameters for the simulation are listed in TABLE 2, and simulator settings are summarized in TABLE 3. A highway scenario is used where road length is 4 km with 3 lanes per direction. The mean and standard deviation of the speed of a vehicle are 113 km/h (70 mph) and

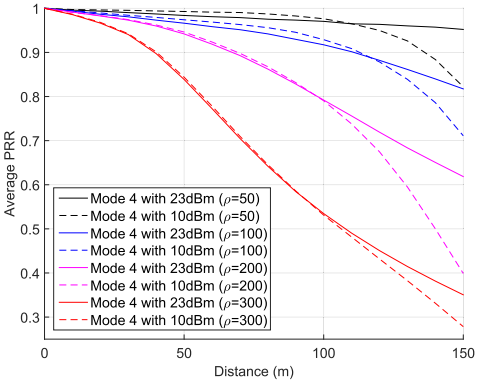


**FIGURE 2.** Impact of transmission power on PRR for the highway scenario. ($T_{\text{CAM}} = 100$ ms).

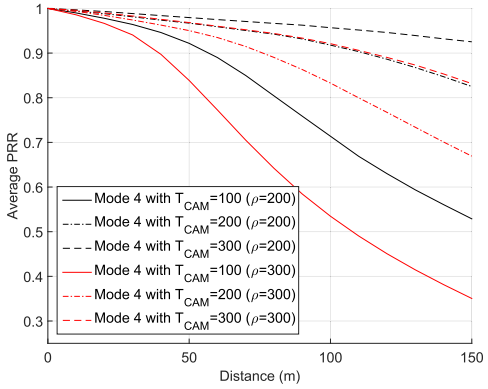


**FIGURE 3.** Impact of message interval on PRR for highway scenarios. ($P_{\text{CAM}} = 23$ dBm).

12.9 km/h (8 mph), respectively, which represent the cruising speed close to the speed limit on highways in the United States. With this settings, we varied the average density of vehicles, $\rho$, from 50 to 300 vehicles/km.

Figures 2 plots the packet reception ratio (PRR) of CAM in C-V2X Mode 4 with varying distances between source and destination vehicles, for vehicle densities of 50, 100, 200, and 300 per km. First of all, higher density results in lower PRR. This is somewhat expected since there will be more transmissions in the channel (collision domain) per unit time given a fixed CAM transmission rate (10 Hz) per vehicle. More interesting result is that lower transmission power results in better PRR up to a certain distance (e.g. 90 m for $\rho = 200$), and after that point, higher power provides better PRR. Furthermore, this break-even distance varies depending on the density. This is because at longer distances, higher power is required for sufficient SINR and thus larger coverage. However at shorter distances, with sufficient signal strength for packet reception, collisions and interference matters more and higher power will only make it worse. This observation is meaningful since the safety implication of PRR is more significant at shorter distances, and a lost message also means longer latency between information updates. Thus, the figure suggests that a fixed transmission power may not be the best strategy for PRR and latency performance; density and distance matters, and there is a trade-off between communication range and contention level affecting PRR.

When the density of vehicles is high, sensing-based scheduling is less effective in avoiding collisions since each available resource is more likely to be already occupied. Furthermore, hidden terminal problem will become more troublesome as channel utilization increases. For example at $\rho = 300$, PRR is below 50% after 100 m, which may be too low for maintaining reasonable quality of service of the system. One possible approach to mitigate this problem would be to reduce the transmit power so that effective density decreases, but the coverage will also decrease, and it will not fundamentally solve the problem. Another more fundamental approach would be to reduce the amount of traffic in the channel so that the resource pool is less occupied and more available. Figures 3 plots the PRR of CAM with varying distances, but now with varying transmission intervals $T_{\text{CAM}}$ of 100, 200, and 300 ms. It shows that as the interval increases, which means reducing the transmission rate, PRR improves significantly thanks to reduced traffic load and interference on the channel.

However, reducing the CAM transmission rate (increasing the message interval) should be done with care since it will increase the latency of CAM updates. At the same time, a lost message also means longer latency between information updates. Thus, message interval should be increased only when it can reduce the average time between successful CAM receptions by improving the PRR. Since it is necessary to consider the requirement of latency or periodicity for each safety application (TABLE 1), we need to address the choice of appropriate message interval carefully. Better would be to combine both the transmission power and message interval and control them jointly and adaptively based on local information in a distributed manner. Based on these observations, we develop an adaptive message interval and power control schemes in the following section.

## V. PROPOSED DESIGN

This section presents the design of *ATOMIC* which addresses the problem identified in the previous section. *ATOMIC* adapts two parameters for this purpose; message interval $T_{\text{CAM}}$ and transmission power $P_{\text{tx}}$, which are the two most impactful parameters in reliable and rapid dissemination of CAMs as noted in [44]. While achieving this goal, we ensure that *ATOMIC* is standard-compliant and backward-compatible.

### A. OVERVIEW OF ATOMIC

To find $T_{\text{CAM}}$ and $P_{\text{tx}}$ that achieves maximum overall average PRR for all vehicles, we need to solve the following optimization problem.

$$\max_{T_{\text{CAM}}, P_{\text{tx}}} \sum_{v_i} \text{PRR}(v_i) \tag{1}$$

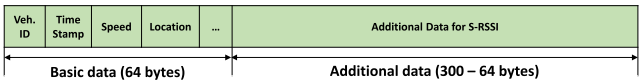


**FIGURE 4.** Proposed CAM configuration for ATOMIC.

$$\text{subject to: } P_C(v_i) \leq 1-\gamma \quad \forall i \tag{2}$$
$$10 \leq P_{\text{tx}}(v_i) \leq 23 \quad \forall i \tag{3}$$
$$T_{\text{CAM}}(v_i) \leq l_t \quad \forall i \tag{4}$$
$$T_{\text{CAM}}(v_i) = n \cdot 100 \quad \forall i \tag{5}$$
$$1 \leq n \leq 10, \text{ and } n \in \mathbb{N}, \tag{6}$$

where $P_C(v_i)$ is the collision probability between the transmitting vehicle $v_i$ and its potential interferer vehicles, and the unit of $P_{\text{tx}}(v_i)$ is dBm. The constraint Eq.(2) guarantees the collision probability to be lower than $1-\gamma$ to avoid excessive collisions. The constraint Eq.(4) implies that the maximum possible value of $T_{\text{CAM}}$ is limited to $l_t$ to prevent average latency from over extending. The appropriate values of $\gamma$ and $l_t$ are given in Section VI.

The constraints Eq.(5) and Eq.(6) allow *ATOMIC* to be backward-compatible with the standard. The SPS algorithm for C-V2X Mode 4 calculates the average of S-RSSI measurements within a sensing period for a representative metric of 'interference level per CR'. Since this averaging procedure is performed every 100 ms, SPS may infer wrong interference level per CR if message interval is not a multiple of 100 ms. As a consequence, a vehicle shall set the resource reservation field according to table 14.2.1-2 in [16] where the resource reservation interval needs to be $n\cdot$100 ms with 1≤n≤10.

Obtaining a closed form solution for the above joint optimization problem is infeasible due to the complexity of mixed integer programming. Alternatively, we propose *ATOMIC* which consists of two sequential steps, (1) message interval control and (2) transmit power control. First, a vehicle chooses an appropriate message interval value to resolve excessive collisions and satisfy the maximum average latency simultaneously. Then, given the selected message interval, the vehicle calculates the optimal transmission power based on the observed S-RSSI statistics. *ATOMIC* chooses a message interval based on the collision probability which is determined by the number of neighbors and the distance from those neighbors. It implies that the message interval control of *ATOMIC* is done regardless of the transmission power of transmitting vehicles although the transmission power of neighbors does influence the number of neighbors. However, the transmission power selection procedure of *ATOMIC* is strongly associated with the message interval. For this reason, *ATOMIC* selects an appropriate message interval and then determines the transmission power. We describe the details of *ATOMIC* in the following sections.

*ATOMIC* is executed during the resource re-selection process in sensing-based SPS as summarized in Algorithm 1.

In *ATOMIC*, each vehicle needs to know the average S-RSSI values of selected CRs (CRs that it had selected for transmission) from all neighbors to obtain the optimal transmission power. To enable this, all vehicles transmit the average S-RSSI values of the CRs that their neighbors will be transmitting on (this information is known from the SCI) using the additional data field in CAM. According to the ETSI standard [18], a CAM contains basic data carrying the status information of the transmitting vehicle and the size of basic data is approximately 64 bytes, which is much smaller than that of a CAM, 300 bytes. The proposed CAM configuration for ATOMIC contains additional information for S-RSSI values as shown in Figure 4. 236 bytes for additional information (or 126 bytes in CAM of 190 bytes) is long enough to contain quantized S-RSSI values of the CRs that their neighbors will be transmitting on. (The number of CRs to transmit is at most the number of neighbors and is less than 90 for $\rho = 300$ in highway scenario.) The quantization level could be determined by the number of neighbors and each vehicle transmits the quantization level using the 'reserved bits' field in SCI. (13 bits is long enough to contain the quantization level.) Using the proposed CAM configuration, each vehicle quantizes the observed S-RSSI values of all CRs which are selected by its neighbors, and transmits them via CAM. This additional procedure helps *ATOMIC* to control the hidden node problem and ensures backward compatibility with the Mode 4 standard. The details of each algorithm for message interval control and power control are presented as follows.

**Algorithm 1** ATOMIC Procedure

```
if SPS counter is 0 then
    select a new resource block CR_N
    procedure MessageIntervalControl
        for All neighbors do
            Calculate the distance from CAM
            Calculate collision probability using Eq. (13)
        return minimum T_CAM satisfying Eq. (14)
    procedure PowerAdaptation
        for All neighbors do
            Collect the average S-RSSI value for CR_N
            Calculate the range of P_tx^T using Eq. (19)
            Calculate the range of P_tx^D using Eq. (22)
        return Most overlapped P_tx among all neighbors
```

### B. MESSAGE INTERVAL CONTROL ALGORITHM

In baseline C-V2X Mode 4, all vehicles persistently broadcast CAMs every 100 ms, which will lead to poor performance in a high-density scenario. This is somewhat obvious; limited resource pool is shared by a large number of vehicles without appropriate adaptation, resulting in excessive collisions and interference. Then, a straightforward solution to resolve this problem is to do rate adaptation by increasing $T_{\text{CAM}}$. Larger message interval could offer a wider choice of resource pools to vehicles, and thus reduce the collision probability. However, larger $T_{\text{CAM}}$ will increase average latency. Thus, a vehicle needs to choose an appropriate $T_{\text{CAM}}$

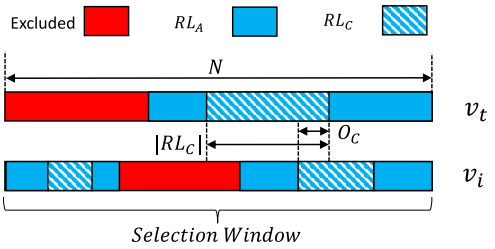


**FIGURE 5.** Classification of resources in C-V2X Mode 4 for two neighboring vehicles.

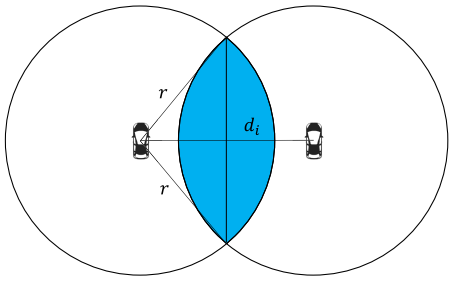


**FIGURE 6.** Illustration of sensing range of two neighboring vehicles at distance $d_i$ and their overlapping region.

carefully considering this trade-off. Our intuition is that small $T_{\text{CAM}}$ may also increase average latency due to higher collision probability and resulting packet losses, and thus there is an optimization point where we can achieve minimum overall latency.

The value of $T_{\text{CAM}}$ that avoids excessive collisions can be obtained by calculating $P_C(T_{\text{CAM}})$, the collision probability between the transmitting vehicle and potential interferer vehicles. There are two kinds of potential interferers: i) vehicles performing simultaneous reselection process with the transmitting vehicle, $v_{res}$, and ii) vehicles that have not been in the awareness distance in the previous time slot, but have newly become 'neighbor vehicles' of the transmitting vehicle, $v_{\text{new}}$. The transmitting vehicle is unaware of the resources selected by $v_{\text{new}}$ since it did not exist in the sensing range of the transmitting vehicle during the sensing period. It means that the collision probability for $v_{\text{new}}$ is same as that for $v_{\text{res}}$ since there is same uncertainty of resource selection for $v_{\text{new}}$ as that for $v_{\text{res}}$. Then, $P_C$ can be calculated by

$$P_C = 1 - \prod_{v_i \in v_{res}, v_{\text{new}}} (1 - p_{col}(v_i)), \tag{7}$$

where $p_{col}(v_i)$ is the probability that a transmitting vehicle and its neighbor vehicles $v_i$ (including $v_{\text{new}}$ and $v_{\text{res}}$) choose the same resource. Here, we utilize the distance between the two as a measure of $p_{col}(v_i)$.

In C-V2X Mode 4, each vehicle creates its own available resource (CR) list, $RL_A$ among total $N = f_{\text{CAM}} T_{\text{CAM}}$ resource pools. Here, $f_{\text{CAM}}$ refers to a possible number of CAMs which can be simultaneously transmitted in the frequency domain. In this work, we assume a typical channel bandwidth of 10 MHz. Channel bandwidth of 10 MHz corresponds to 50 pairs of RBs per subframe. Each transport block (TB) has an associated control message, called SCI, which requires 2 pairs of RBs. It means that the number of required RBs to transmit SCI varies according to that of TBs which is determined by MCS level. The position of RBs carrying SCI also varies according to MCS level. For simplicity, we assume a non-adjacent Physical Sidelink Control CHannel (PSCCH) and Physical Sidelink Shared CHannel (PSSCH) configuration which means that specific resources (10 pairs of RBs) are reserved for PSCCH carrying SCI and the remaining are used by PSSCH carrying data. Under these assumptions, the value of $f_{\text{CAM}}$ is 1 with MCS 4, 2 with MCS 7, and 4 with MCS 14. Then, each vehicle lists the set of candidate CRs, $RL_C$, and randomly selects the CR to use among $|RL_C| = 0.2N$ CRs. Consequentially, the probability that two neighboring vehicles select the same CR to use depends on the number of overlapped candidate CRs, $O_C$. The concept of $RL_A$, $RL_C$, and $O_C$ is demonstrated in Figure 5. Then, $p_{col}(v_i)$ can be expressed by,

$$p_{col}(v_i) = \frac{O_C(v_i)}{|RL_C|^2} = \frac{O_C(v_i)}{(0.2 f_{\text{CAM}} T_{\text{CAM}})^2}, \tag{8}$$

where $O_C(v_i)$ is the number of overlapped candidate resources between the transmitting vehicle and its neighbor $v_i$, and $|RL_C| = 0.2N = 0.2 f_{\text{CAM}} T_{\text{CAM}}$.

However, the derivation of $O_C$ in an exact closed-form is not feasible [34]. To deal with this, we assume that $O_C(v_i)$ is proportional to the ratio of overlapped sensing range between the two vehicles to its own sensing range. Figure 6 illustrates that the ratio $x_i$ can be easily calculated by

$$x_i = \frac{2}{\pi} \arccos \frac{d_i}{2r} - \frac{d_i}{\pi r} \sqrt{1 - \frac{d_i^2}{4r^2}}, \tag{9}$$

where $d_i$ is the distance between the transmitting vehicle and interferer vehicle, and $r$ is the sensing range, which is common for all vehicles.

Now, we calculate the values of $O_C(v_i)$ for $x_i = 1$ and $x_i = 0$. When $x_i = 1$, the distance between the two vehicles is zero so that sensing results are all the same. It means

$$O_C(x_i = 1) = |RL_C|. \tag{10}$$

When $x_i = 0$, the transmitting vehicle and $v_i$ do not have any common neighbor. It means that the resource selection procedure of the two vehicles becomes independent process. Using this independence property, the expectation of $O_C(x_i = 0)$ can be derived by

$$\begin{aligned} E[O_C(x_i = 0)] &= \sum_{i=1}^{|RL_C|} i \times \frac{\binom{N-|RL_C|}{|RL_C|-i}\binom{|RL_C|}{i}}{\binom{N}{|RL_C|}} \\ &= \frac{|RL_C|^2}{N} = 0.04N, \end{aligned} \tag{11}$$

where $\binom{n}{k}$ is the combination operation.

From the assumption that $O_C(v_i)$ is proportional to $x_i$, $O_C(v_i)$ can be expressed as,

$$O_C(v_i) = (O_C(x_i = 1) - E[O_C(x_i = 0)])x_i + E[O_C(x_i = 0)]. \tag{12}$$

Using Eq. (8), Eq. (10), Eq. (11), and Eq. (12), we can rewrite $p_{col}(v_i)$ in terms of $T_{\text{CAM}}$ as follows:

$$\begin{aligned} p_{col}(v_i) &\approx \frac{|RL_C| - 0.04N}{|RL_C|^2} x_i + \frac{0.04N}{|RL_C|^2} \\ &= \frac{0.2N - 0.04N}{0.04N^2} x_i + \frac{0.04N}{0.04N^2} \\ &= \frac{4}{N} x_i + \frac{1}{N} = \frac{4}{f_{\text{CAM}} T_{\text{CAM}}} x_i + \frac{1}{f_{\text{CAM}} T_{\text{CAM}}}. \end{aligned} \tag{13}$$

Now, we can calculate $P_C$ as a function of $T_{\text{CAM}}$ by plugging Eq. (9) and Eq. (13) into Eq. (7). Using this, we design the message interval control algorithm which finds the minimum $T_{\text{CAM}}$ that guarantees the collision probability to be lower than $1 - \gamma$ to avoid excessive collisions. In other words, the proposed message interval control algorithm chooses minimum $T_{\text{CAM}} \leq l_t$ satisfying

$$1 - P_C = \prod_{v_i \in v_{res}, v_{\text{new}}} (1 - p_{col}(v_i)) \geq \gamma. \tag{14}$$

Here, we define the maximum possible $T_{\text{CAM}}$ as $l_t$ to prevent average latency from overextending.

### C. POWER ADAPTATION ALGORITHM

Power control in V2X communication is a challenging issue due to mobility, distributed and peer-to-peer characteristics, and nature of message broadcasting. For uplink power control in the legacy LTE network, the base station sends transmit power control (TPC) command to UEs so that the received power is maintained at a desired level. However, such TPC command or feedback is not available in C-V2X over sidelink since the receiver to provide feedback is not particularly designated in sidelink transmissions for V2X. Furthermore, we have shown in Section IV that higher transmission power may only deteriorate PRR in a dense network by increasing interference level while it may transmit messages farther in a sparse environment. Thus, to apply open-loop power control for C-V2X over sidelink based on these observations, we resort to take channel sensing measurements into considerations for transmission power decision for C-V2X Mode 4.

Figure 7 shows the impact of transmission power control. While the main purpose of the previous message interval control algorithm is to reduce persistent packet collisions, this power control algorithm addresses interference mitigation between contender vehicles which collide with each other from selecting the same resource to use. In this case, we need to consider the capture effect where only the stronger of two signals at or near the same frequency will be demodulated. Utilizing this capture effect, a transmitting vehicle derives the range of its transmission power which guarantees a message reception for each neighbor. Here, neighbor's message reception can be divided into 2 cases: i) reception of other dominant

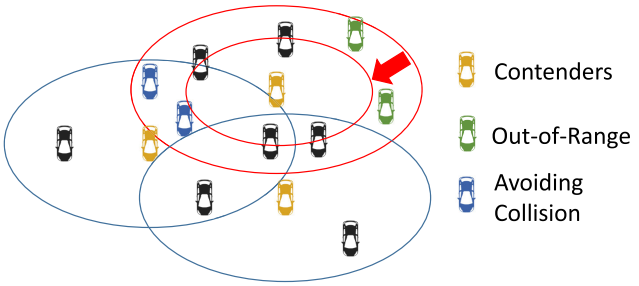


**FIGURE 7.** Impact of transmission power. If the transmitting vehicle reduces its transmission power, the number of out-of-range vehicles increases whereas that of vehicles suffering collisions decreases.

neighbor's message, and ii) reception of the transmitting vehicle's message. In cooperative awareness services, since the most important thing is not individual throughput but overall system reliability, we need to consider both cases as equally important. So in our proposed algorithm, the transmitting vehicle needs to count the number of messages expected to be successfully received for each $P_{\text{tx}}$, and then chooses the $P_{\text{tx}}$ having the highest expectation of successful message reception. The details of our power adaptation algorithm are as follows.

*Estimation of the Strongest Vehicle:* For a specific receiver, we consider a scenario where there are two or more vehicles selecting the same resource block to transmit CAMs on it. Among them, we define the transmitter vehicle who has the highest received signal strength as $D$, and its received signal strength as $R_D$. Received signal strength from the other transmitter vehicle is defined as $R_I$. Then, the RSSI value of the receiver for the collided resource block can be given by,

$$RSSI = R_D + R_I + N_0, \tag{15}$$

where $N_0$ is the noise level. The receiver can successfully decode the message of $D$ if the signal-to-interference-plus-noise ratio (SINR) is larger than $\eta$, where $\eta$ is the minimum SINR threshold to successfully decode messages which can be obtained by applying the LTE specifications in [45]. Then, if $R_D \geq \frac{\eta}{\eta+1} RSSI$, the SINR for $D$ satisfies

$$SINR_D = \frac{R_D}{R_I + N_0} \geq \eta. \tag{16}$$

Then, if we adopt $\beta \geq 1$, which represents SINR margin, the received signal power of the strongest vehicle whose messages can be successfully decoded by the capture effect can be estimated by

$$R_D = \frac{\beta\eta}{\beta\eta + 1} RSSI. \tag{17}$$

By applying this estimation, the transmission power range of the transmitting vehicle satisfying following two cases can be derived.

*Reception of the Transmitting Vehicle's Message:* A specific receiver successfully receives the transmitting vehicle's

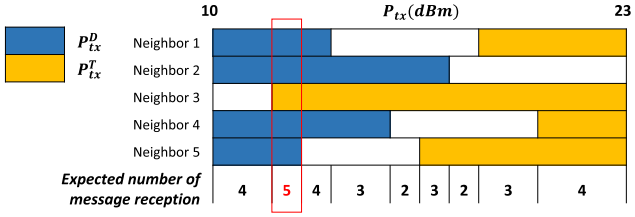


**FIGURE 8.** Example of the optimal transmission power selection procedure in the power adaptation algorithm.

message if the transmission power range of the transmitting vehicle, $P_{\text{tx}}^{T}$, satisfies

$$P\left[\frac{P_{\text{tx}}^{T}}{SH \cdot PL \cdot RSSI} \geq \eta\right] \geq \alpha, \tag{18}$$

where $SH$ and $PL$ are the shadowing coefficient and path-loss, respectively, $RSSI$ is measured by the receiver for the collided resource block, and $\alpha$ is the guaranteed message reception probability under fading environments. If we consider log-normal shadowing, this becomes

$$\frac{1}{2} + \frac{1}{2}\,\text{erf}\left(\frac{\ln(\frac{P_{\text{tx}}^{T}}{PL \cdot RSSI \cdot \eta})}{\sigma\sqrt{2}}\right) \geq \alpha, \tag{19}$$

where $\sigma$ is the shadowing variance in TABLE 3 and $\text{erf}(x)$ is the Gauss error function, which is defined as

$$\text{erf}(x) = \frac{2}{\sqrt{\pi}}\int_{0}^{x} e^{-t^2}dt. \tag{20}$$

*Reception of other neighbor's message:* A specific receiver successfully receives other neighbor's message having the highest received signal strength if the transmission power range of the transmitting vehicle, $P_{\text{tx}}^{D}$, satisfies

$$P\left[\frac{\frac{\beta\eta}{\beta\eta+1}SH \cdot RSSI}{\frac{P_{\text{tx}}^{D}}{PL} + \frac{1}{\beta\eta+1}SH \cdot RSSI} \geq \eta\right] \geq \alpha. \tag{21}$$

With the assumption of log-normal shadowing, this becomes

$$\frac{1}{2} - \frac{1}{2}\,\text{erf}\left(\frac{\ln(\frac{P_{\text{tx}}^{D}(\beta\eta+1)}{PL \cdot RSSI \cdot (\beta-1)})}{\sigma\sqrt{2}}\right) \geq \alpha. \tag{22}$$

*Selection of the optimal transmission power:* Based on the range of $P_{\text{tx}}^{T}$ and $P_{\text{tx}}^{D}$ for all neighbor vehicles, the transmitting vehicle compares them and chooses the most overlapped $P_{\text{tx}}$ value among all neighbors as in Figure 8. It means that the value guarantees the highest expectation of successful message reception. Through the process, transmit power is adaptively determined based on S-RSSI statistics that indicate the level of interference from candidate interferers.

## VI. EVALUATION

We evaluate and compare the performance of *ATOMIC* against C-V2X Mode 4 standard SPS using trace-driven simulations.

### A. SIMULATION SETUP AND EVALUATION METRICS

To generate realistic road topology and vehicle mobility, we utilize the SUMO simulator [46] which generates traces that can be fed as an input to the MATLAB-based LTEV2Vsim simulator [42]. We use two distinct environments for our simulations: (1) highway scenario, and (2) urban environment in Manhattan city. For each setting, we run the simulations five times and the simulation time is 90 seconds for each episode.

We use the same settings used in Section IV along with simulation parameters of $\alpha = 0.921$, $\beta = 1.2$, $\gamma = 0.95$, and $l_t = 500$. The reason for selecting these parameter values are as follows: Since $\text{erf}(x)$ is saturated when $x > 1$ and thus it has a negligible gain as $x > 1$ increases, we chose $\alpha = 1/2 + 1/2\,\text{erf}(1) = 0.921$ from Eq. (19). The maximum allowed message interval $l_t$ is chosen as $5 \cdot 100$ ms from the fact that the minimum number of consecutive packet transmissions using the same resources in Mode 4 is 5 as mentioned in Section II-A. It means that if a vehicle selects the same resources as others, it suffers collisions for at least 500 ms. We select 20% and 5% for the margin of SINR and collision, respectively, which translates to $\beta = 1.2$ and $\gamma = 0.95$.

The following performance metrics are used for evaluation.

- **Average PRR** is the average ratio of the correctly decoded CAMs over the total number of transmitted CAMs.
- **Tail update delay (UD)** is the worst 1% value of UD. Given a transmitter and receiver pair, UD is defined as the time gap between two correctly received consecutive CAMs from the same neighbor vehicle. Tail UD can be interpreted as the time for the vehicle suffering from the worst channel condition to obtain up-to-date information from its neighbors.
- **CAM range ($r_{\text{CAM}}$)** is the maximum distance at which the achieved PRR exceeds the minimum acceptable PRR, $\text{PRR}_{TH}$. This metric has already been considered in the literature, and the threshold is typically set to 0.9 [23], [47]–[49]. For this reason, we also set $\text{PRR}_{TH}$ to 0.9 in our evaluation.

### B. AVERAGE PRR

We first simulate the same highway scenario as introduced in Section IV. The speed of a vehicle follows a normal distribution where the mean and standard deviation are 113 km/h and 12.9 km/h, respectively. Figure 9 plots the PRR of *ATOMIC* compared to the power control algorithm in [33] as well as C-V2X Mode 4 standard with MCS 4 and $p_k = 0$. As we mentioned in Section III, there is only one prior work (to the best of our knowledge) which is standard-compliant with C-V2X Mode 4, and that is the power control scheme in [33]. To compare *ATOMIC* with a standard-compliant algorithm, we choose [33] as a benchmark. From the data in [50] and [51], traffic volume in Gyeongbu Expressway is 120 vehicles per km during day time. So, we compare the performance when the vehicle densities are 100, 200, and 300 vehicles per

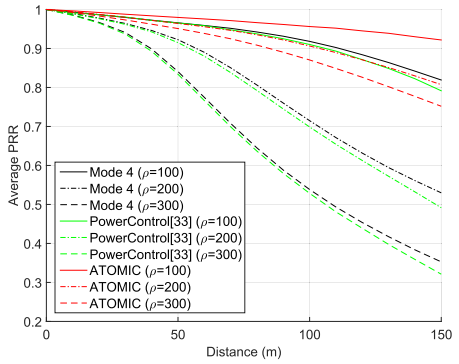


**FIGURE 9.** Comparison of C-V2X Mode 4 standard, power control scheme in [33] and *ATOMIC* in terms of average PRR for highway scenarios.

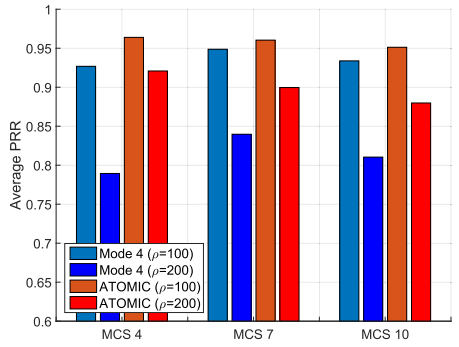


**FIGURE 10.** Average PRR of standard C-V2X Mode 4 and *ATOMIC* for various MCS levels.

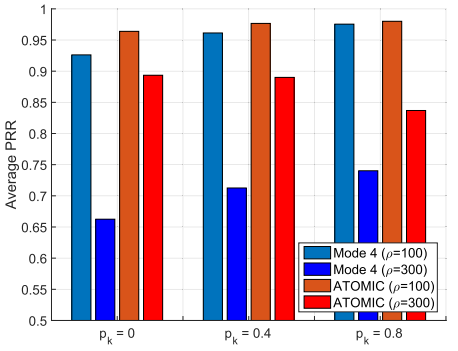


**FIGURE 11.** Average PRR of standard C-V2X Mode 4 and *ATOMIC* for various $p_k$ values.

**FIGURE 12.** Map of the Manhattan scenario which contains building and speed limit information. The total area is 22 km$^2$.

km. In the sparse scenario with $\rho = 100$, where the collision probability and interference levels are low, *ATOMIC* tends to select high transmission power and low $T_{\text{CAM}}$. Since this behavior is similar to Mode 4 and the power adaptation in [33], it does not show much of performance gain compared to those as shown in Figure 9. However, as $\rho$ increases to create denser environments, vehicle UEs suffer more collisions and interference. Due to huge contention with many vehicles, Figure 9 shows severe performance degradation for both Mode 4 standard algorithm and the power control algorithm in [33]. It means that an algorithm which adjusts only the transmission power does not sufficiently resolve contention. They merely obtain slightly better PRR at shorter distances while sacrificing coverage. On the other hand, through the message interval control to resolve contention and the power adaptation to mitigate mutual interference, *ATOMIC* achieves significantly better PRR in a dense network as shown in Figure 9.

Figure 10 shows the impact of MCS level on average PRR for 3GPP standard and *ATOMIC*. From now on, we focus on the comparison of performance between Mode 4 and *ATOMIC* since that of power control scheme in [33] is similar to Mode 4. Here, MCS indices are based on table 8.6.1-1 in 3GPP TS 36.213 [16]. MCS 4, 7, and 10 use the same modulation order of QPSK, but different effective coding rate of 0.337, 0.577, and 0.820, respectively. In general, higher MCS increases the required minimum SINR $\eta$, but this provides more available resource pools for CAMs, which results in a lower collision probability. It means that high MCS may help to decrease the collision probability while low MCS is suitable for contention-free environment with limited transmission power, and this trend is verified in [28]. As a result, Mode 4 standard which may suffer from limited resource pool provides the highest PRR with MCS 7. On the other hand, since *ATOMIC* resolves highly contended scenarios by reducing the effective density, lowest MCS level is the best due to raised $\eta$.

We also investigate the impact of $p_k$ on average PRR for Mode 4 and *ATOMIC* as shown in Figure 11. The keep probability, $p_k$, is the key parameter which determines the duration of maintaining the same SPS allocation. Higher $p_k$ decreases the number of $v_{res}$, and thus reduces the number of contended vehicles selecting resources simultaneously, while wrong resource selections are maintained for longer time. It means that high $p_k$ may help to decrease the collision probability. In consequence, Mode 4 provides the highest PRR with $p_k = 0.8$. However, since *ATOMIC* enhances resource selection procedure of C-V2X Mode 4 by decreasing the collision probability, more frequent resource selection (low $p_k$) helps to find up-to-date optimal transmission power and message interval according to rapidly changing environments and quickly recover from wrong resource selections. This is why highest performance gain is obtained when $p_k = 0$.

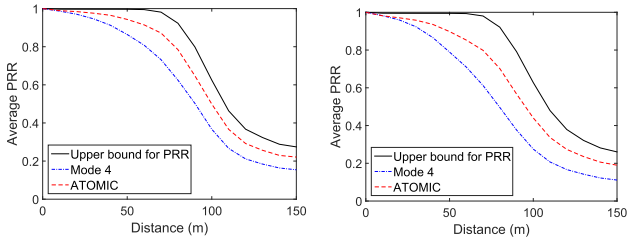


(a) $\rho = 50$ vehicles/km (b) $\rho = 100$ vehicles/km

**FIGURE 13.** Average PRR of C-V2X Mode 4 standard and *ATOMIC* for Manhattan scenario.

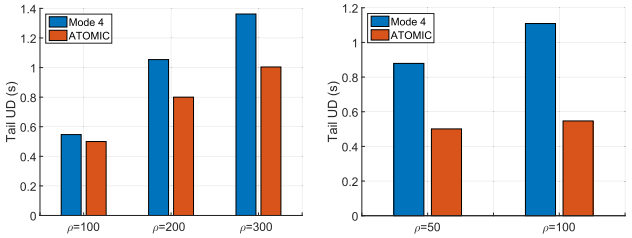


(a) Highway scenario (b) Manhattan scenario

**FIGURE 14.** Comparison of C-V2X Mode 4 standard and *ATOMIC* in terms of worst 1% update delay (tail UD).

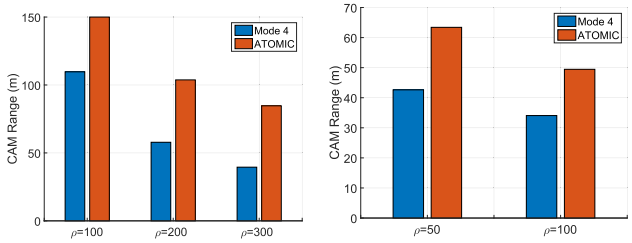


(a) Highway scenario (b) Manhattan scenario

**FIGURE 15.** Comparison of C-V2X Mode 4 standard and *ATOMIC* in terms of effective CAM range (awareness distance).

Next, to verify the performance enhancement of *ATOMIC* in a realistic urban scenario, map of Manhattan, New York City is used. Since the traffic is more likely to be locally crowded due to intersections and traffic lights, *ATOMIC* is expected to be necessary and well-suited for such urban scenarios. For this purpose, we export a map of Manhattan from OpenStreetMap[1] including building and road information, which is shown in Figure 12. The speed of a vehicle follows a truncated normal distribution where the maximum and minimum speeds are 120% and 80% of the average speed, respectively. Average speed is determined by the speed limit of the road where each vehicle travels. So, it varies according to each vehicle's position.

Figure 13 plots the average PRR for the Manhattan scenario with densities of 50 and 100 vehicles/km. These values imply the same vehicle density per lane as the highway scenario with $\rho = 100$ and $\rho = 200$, respectively, since from OpenStreetMap, the roads in Manhattan are 3 lanes on average, which are half of those in highway scenario. Average PRR trend for the Manhattan scenario is similar to that of highway scenarios, but the overall PRR is lower. It is due to the fact that an urban scenario is an almost non line-of-sight (NLOS) environment due to buildings and intersections. To isolate the performance degradation caused by NLOS and collision, we plot the upper bound of average PRR which can be obtained by assuming an interference-free environment. So, the gap between this upper bound and the PRR results indicate the effect of interference and collision on the average system PRR. As shown in Figure 13, *ATOMIC* mitigates almost half of total CAM losses due to interference and collision.

### C. TAIL UD

Figure 14 compares the tail UD performance of two algorithms. Since UD quantifies how long a vehicle does not receive any CAM from its neighbor, tail UD is important and meaningful for reliable cooperative awareness services. Although *ATOMIC* uses higher message intervals than Mode 4 standard, it exhibits lower tail UD since it mitigates collision and thus has better chance of receiving what has been sent. It implies that *ATOMIC* improves the performance of the worst vehicle as well as the overall system performance on average. Obviously, the vehicles who experience severe collisions need longer time to escape the situation as the environment becomes denser, and this trend is observed for both highway and Manhattan scenarios in Figure 14(a) and Figure 14(b), respectively.

### D. CAM RANGE

Effective CAM range results for the standard and *ATOMIC* algorithms are shown in Figure 15. It quantifies the maximum distance to guarantee reliable transmission of CAMs. In both highway and Manhattan environments, *ATOMIC* achieves significantly longer communication range, thus awareness distance. For example, CAM range of *ATOMIC* is almost twice that of Mode 4 standard for the highway scenario with $\rho = 300$. Furthermore, we can infer the effect of NLOS by comparing Figure 15(a) and Figure 15(b) since an urban environment is expected to have more NLoS links compared to the highway case. They show significantly decreased CAM range for the Manhattan case, most likely due to the high carrier frequency of 5.9 GHz.

## VII. CONCLUSION

C-V2X is one of the key technologies for autonomous vehicles, vehicular networks, and smart transportation services. In this work, we identified that C-V2X standard needs to be improved for a highly dense environment due to severe collisions and interference. To address the problem, we proposed *ATOMIC* for C-V2X Mode 4 which helps vehicles to adapt their transmission power and message interval jointly according to the density of neighboring vehicles. *ATOMIC* exploits S-RSSI values to infer crowdedness in the proximity, estimates the expected collision probability as a function of message interval, and infers the expected PRR value for

[1] OpenStreetMap, https://www.openstreetmap.org/

various transmission powers. Evaluation via extensive simulation verified that the proposed algorithm enhances conventional Mode 4 in both urban and highway scenarios.

We have taken a stochastic approach in this work where each vehicle makes its decision based on estimated collision probability. As future work, we plan to adopt machine learning techniques to enable each vehicle to predict its neighbors' decision and find the optimal resource selection policy such as a recent study leveraging a deep learning tool for vehicular communications [52]. We will also investigate utilizing roadside units [53] for resource scheduling of V2V messages.

## ACKNOWLEDGMENT

An earlier version of a part of this work was introduced in the first author's own Ph.D. thesis [1] as one of his several research work. However, this article has been significantly revised, modified, and extended from that version.

## REFERENCES

[1] B. Kang, "Intelligent resource management for reliable sidelink communications in cellular networks," Doctoral dissertation, Seoul Nat. Univ., Seoul, South Korea, 2020. [Online]. Available: http://s-space.snu.ac.kr/handle/10371/168031

[2] *Dedicated Short Range Communications (DSRC) Message Set Dictionary*, Standard Doc J2735, SAE International, Nov. 2009.

[3] *Standard Specification for Telecommunications and Information Exchange Between Roadside and Vehicle Systems5 GHz Band Dedicated Short Range Communications (DSRC) Medium Access Control (MAC) and Physical Layer (PHY) Specifications*, Standard ASTM E2213-03, ASTM International, Aug. 2003.

[4] J. B. Kenney, "Dedicated short-range communications (DSRC) standards in the united states," *Proc. IEEE*, vol. 99, no. 7, pp. 1162–1182, Jul. 2011.

[5] *Standard for Wireless Access in Vehicular Environments (WAVE)—Architecture*, IEEE Standard 1609.0-2013, 2013.

[6] *Standard for Wireless Access in Vehicular Environments (WAVE)—Security Services for Applications an d Management Messages*, IEEE Standard 1609.2-2016, 2016.

[7] *Standard for Wireless Access in Vehicular Environments (WAVE)–Multi-Channel Operation*, IEEE Standard 1609.4-2016, 2016.

[8] S. Eichler, "Performance evaluation of the IEEE 802.11p WAVE communication standard," in *Proc. IEEE 66th Veh. Technol. Conf.*, Sep. 2007, pp. 2199–2203.

[9] K. Bilstrup, E. Uhlemann, E. G. Strom, and U. Bilstrup, "Evaluation of the IEEE 802.11p MAC method for vehicle-to-vehicle communications," in *Proc. IEEE 68th Veh. Technol. Conf. (VTC-Fall)*, Calgary, AB, Canada, Sep. 2008, pp. 1–5.

[10] *Evolved Universal Terrestrial Radio Access (E-UTRA) and Evolved Universal Terrestrial Radio Access Network (E-UTRAN); Overall Description; Stage 2*, document TS 36.300 V14.1.0, 3GPP, Dec. 2016.

[11] *Scenarios, Requirements and KPIs for 5G Mobile and Wireless Systems*, D1.1, METIS, Europe, May 2013.

[12] *Technical Specification Group Radio Access Network; NR; Physical Channels and Modulation*, document TS 38.211 V16.0.0, 3GPP, Dec. 2019.

[13] *Technical Specification Group Radio Access Network; NR; Physical Layer Procedures for Control*, document TS 38.213 V16.0.0, 3GPP, Dec. 2019.

[14] *Technical Specification Group Radio Access Network; NR; Physical Layer Procedures for Data*, document TS 38.214 V16.0.0, 3GPP, Dec. 2019.

[15] *Technical Specification Group Radio Access Network; NR; Study on NR Vehicle-to-Everything (V2X)*, document TS 38.885 V16.0.0, 3GPP, Mar. 2019.

[16] *Technical Specification Group Radio Access Network; Evolved Universal Terrestrial Radio Access (E-UTRA); Physical Layer Procedures*, document TS 36.213 V14.7.0, 3GPP, Jun. 2018.

[17] *Technical Specification Group Radio Access Network; Evolved Universal Terrestrial Radio Access (E-UTRA); Medium Access Control (MAC) Protocol Specification*, document TS 36.321 V14.7.0, 3GPP, Jul. 2018.

[18] *Intelligent Transport System (ITS); Vehicular Communications; Basic Set of Applications; Part 2: Specification of Cooperative Awareness Basic Service*, document TS 302 637-2 V1.3.2, ETSI, Nov. 2011.

[19] P. M. d'Orey and M. Boban, "Empirical evaluation of cooperative awareness in vehicular communications," in *Proc. IEEE 79th Veh. Technol. Conf. (VTC Spring)*, May 2014, pp. 1–5.

[20] *Study on LTE Support for V2X Services*, document TR 22.885 V14.0.0, 3GPP, Dec. 2015.

[21] *Intelligent Transport System (ITS); Vehicular Communications; Basic Set of Applications; Definitions*, document TR 102 638 V1.1.1, ETSI, Jun. 2009.

[22] *Vehicle Safety Communications Project Task 3 Final Report–Identify Intelligent Vehicle Safety Applications Enabled by DSRC*, NHTSA, Washington, DC, USA, Mar. 2005.

[23] A. Bazzi, B. M. Masini, and A. Zanella, "Cooperative awareness in the Internet of vehicles for safety enhancement," *EAI Endoresed Trans. Internet Things*, vol. 3, no. 9, pp. 1–10, Aug. 2017.

[24] R. Molina-Masegosa and J. Gozalvez, "System level evaluation of LTE-V2 V mode 4 communications and its distributed scheduling," in *Proc. IEEE 85th Veh. Technol. Conf. (VTC Spring)*, Sydney, NSW, Australia, Jun. 2017, pp. 1–5.

[25] R. Molina-Masegosa and J. Gozalvez, "LTE-V for sidelink 5G V2X vehicular communications: A new 5G technology for short-range Vehicle-to-Everything communications," *IEEE Veh. Technol. Mag.*, vol. 12, no. 4, pp. 30–39, Dec. 2017.

[26] M. Wang, M. Winbjork, Z. Zhang, R. Blasco, H. Do, S. Sorrentino, M. Belleschi, and Y. Zang, "Comparison of LTE and DSRC-based connectivity for intelligent transportation systems," in *Proc. IEEE 85th Veh. Technol. Conf. (VTC Spring)*, Sydney, NSW, Australia, Jun. 2017, pp. 1–5.

[27] T. V. Nguyen, P. Shailesh, B. Sudhir, G. Kapil, L. Jiang, Z. Wu, D. Malladi, and J. Li, "A comparison of cellular vehicle-to-everything and dedicated short range communication," in *Proc. IEEE Veh. Netw. Conf. (VNC)*, Nov. 2017, pp. 101–108.

[28] A. Bazzi, G. Cecchini, A. Zanella, and B. M. Masini, "Study of the impact of PHY and MAC parameters in 3GPP C-V2 V mode 4," *IEEE Access*, vol. 6, pp. 71685–71698, Nov. 2018.

[29] L. F. Abanto-Leon, A. Koppelaar, and S. H. de Groot, "Enhanced C-V2X mode-4 subchannel selection," in *Proc. IEEE 88th Veh. Technol. Conf. (VTC-Fall)*, Chicago, IL, USA, Aug. 2018, pp. 1–5.

[30] *On-board System Requirements for V2V Safety Communications*, Standard Doc J2945/1, SAE International, Mar. 2016.

[31] A. Mansouri, V. Martinez, and J. Harri, "A first investigation of congestion control for LTE-V2X mode 4," in *Proc. 15th Annu. Conf. Wireless On-Demand Netw. Syst. Services (WONS)*, Wengen, Switzerland, Jan. 2019, pp. 56–63.

[32] B. Toghi, M. Saifuddin, Y. P. Fallah, and M. O. Mughal, "Analysis of distributed congestion control in cellular vehicle-to-everything networks," in *Proc. IEEE 90th Veh. Technol. Conf. (VTC-Fall)*, Honolulu, HI, USA, Sep. 2019, pp. 1–7.

[33] B. Kang, S. Jung, and S. Bahk, "Sensing-based power adaptation for cellular V2X mode 4," in *Proc. IEEE Int. Symp. Dyn. Spectr. Access Netw. (DySPAN)*, Oct. 2018, pp. 1–4.

[34] M. Gonzalez-Martin, M. Sepulcre, R. Molina-Masegosa, and J. Gozalvez, "Analytical models of the performance of C-V2X mode 4 vehicular communications," *IEEE Trans. Veh. Technol.*, vol. 68, no. 2, pp. 1155–1166, Feb. 2019.

[35] A. Nabil, K. Kaur, C. Dietrich, and V. Marojevic, "Performance analysis of sensing-based semi-persistent scheduling in C-V2X networks," in *Proc. IEEE 88th Veh. Technol. Conf. (VTC-Fall)*, Aug. 2018, pp. 1–5.

[36] V. Mannoni, V. Berg, S. Sesia, and E. Perraud, "A comparison of the V2X communication systems: ITS-G5 and C-V2X," in *Proc. IEEE 89th Veh. Technol. Conf. (VTC-Spring)*, Apr. 2019, pp. 1–5.

[37] K. Z. Ghafoor, M. Guizani, L. Kong, H. S. Maghdid, and K. F. Jasim, "Enabling efficient coexistence of DSRC and C-V2X in vehicular networks," *IEEE Wireless Commun.*, vol. 27, no. 2, pp. 134–140, Apr. 2020.

[38] *Basic System Profile*, document RS 2037 V1.3.0, C2C-CC, Aug. 2018.

[39] *Road Transport and Traffic Telematics–Dedicated Short Range Communication–DSRC Data Link Layer: Medium Access and Logical Link Control*, document EN 12795, CEN, Mar. 2003.

[40] *Electromagnetic Compatibility and Radio Spectrum Matters (ERM); Road Transport and Traffic Telematics (RTTT); DSRC Transmission Equipment (500 kbit/s/250 kbit/s) Operating in the 5, 8 GHz Industrial, Scientific and Medical (ISM) Band*, document EN 300 674-2-2 V2.0.3, ETSI, Mar. 2016.

[41] *Intelligent Transport System (ITS); Mitigation Techniques to Avoid Interference Between European CEN DSRC Equipment and ITS Operating in the 5 GHz Frequency Range*, document TS 102 792 V1.2.1, ETSI, Jun. 2015.
[42] G. Cecchini, A. Bazzi, B. M. Masini, and A. Zanella, "LTEV2Vsim: An LTE-V2V simulator for the investigation of resource allocation for cooperative awareness," in *Proc. 5th IEEE Int. Conf. Models Technol. Intell. Transp. Syst. (MT-ITS)*, Jun. 2017, pp. 80–85.
[43] *Technical Specification Group Radio Access Network; Study on LTE-Based V2X Services*, document TR 36.885 V14.0.0, 3GPP, Jul. 2016.
[44] Y. P. Fallah, N. Nasiriani, and H. Krishnan, "Stable and fair power control in vehicle safety networks," *IEEE Trans. Veh. Technol.*, vol. 65, no. 3, pp. 1662–1675, Mar. 2016.
[45] A. Bazzi, B. M. Masini, and A. Zanella, "How many vehicles in the LTE-V2 V awareness range with half or full duplex radios?" in *Proc. 15th Int. Conf. ITS Telecommun. (ITST)*, May 2017, pp. 1–6.
[46] *SUMO Simulator*. Accessed: Feb. 2020. [Online]. Available: http://sumo.dlr.de/
[47] M. Boban and P. M. d'Orey, "Exploring the practical limits of cooperative awareness in vehicular communications," *IEEE Trans. Veh. Technol.*, vol. 65, no. 6, pp. 3904–3916, Jun. 2016.
[48] J. Breu, A. Brakemeier, and M. Menth, "A quantitative study of cooperative awareness messages in production VANETs," *EURASIP J. Wireless Commun. Netw.*, vol. 2014, no. 1, p. 98, Dec. 2014.
[49] M. Boban and P. M. d'Orey, "Exploring the practical limits of cooperative awareness in vehicular communications," *IEEE Trans. Veh. Technol.*, vol. 65, no. 6, pp. 3904–3916, Jun. 2016.
[50] Expressway Coporation, South Korea. (2019). *Statistical Information on Traffic Volume in South Korea Expressway*. [Online]. Available: http://data.ex.co.kr/portal/traffic/trafficByIc
[51] T. Kim, Y. Park, H. Kim, and D. Hong, "Cooperative superposed transmission in cellular-based V2 V systems," *IEEE Trans. Veh. Technol.*, vol. 68, no. 12, pp. 11888–11901, Dec. 2019.
[52] S. Moon, H. Kim, and I. Hwang, "Deep learning-based channel estimation and tracking for millimeter-wave vehicular communications," *J. Commun. Netw.*, vol. 22, no. 3, pp. 177–184, Jun. 2020.
[53] J. Heo, B. Kang, J. M. Yang, J. Paek, and S. Bahk, "Performance-cost tradeoff of using mobile roadside units for V2X communication," *IEEE Trans. Veh. Technol.*, vol. 68, no. 9, pp. 9049–9059, Sep. 2019.

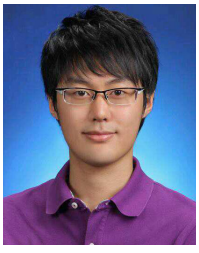

**BYUNGJUN KANG** received the B.S. and M.S. degrees in electrical engineering from the Korea Advanced Institute of Science and Technology (KAIST), in 2010 and 2013, respectively, and the Ph.D. degree from the School of Computer Science and Electrical Engineering, Seoul National University, in 2020. He currently works with Samsung Research, the advanced Research and Development hub of Samsung Electronics. His research interests include information theory and resource management in wireless networks, including device-to-device (D2D) and vehicle-to-everything (V2X) communications.

**JINMO YANG** received the B.S. degree in electronic engineering from Hanyang University, in 2018. He is currently pursuing the Ph.D. degree in electrical and computer engineering with Seoul National University. His research interests include vehicle to everything (V2X) communication and on-path computing to realize neural network services for 6G networks.

**JEONGYEUP PAEK** (Senior Member, IEEE) received the B.S. degree in electrical engineering from Seoul National University, in 2003, and the M.S. degree in electrical engineering and the Ph.D. degree in computer science from the University of Southern California (USC), in 2005 and 2010, respectively. He was a member of the Networked Systems Laboratory, USC, led by Dr. Ramesh Govindan. He worked at Deutsche Telekom Inc., Research and Development Labs, USA, as a Research Intern, in 2010, and then joined Cisco Systems Inc., in 2011, where he was the Technical Leader in the Internet of Things Group, Connected Energy Networks Business Unit (formerly the Smart Grid Business Unit). In 2014, he was an Assistant Professor with the Department of Computer Information Communication, Hongik University. He is currently an Associate Professor with the School of Computer Science and Engineering, Chung-Ang University, Seoul, Republic of Korea.

**SAEWOONG BAHK** (Senior Member, IEEE) received the B.S. and M.S. degrees in electrical engineering from Seoul National University (SNU), in 1984 and 1986, respectively, and the Ph.D. degree from the University of Pennsylvania, in 1991. He is currently a Professor with SNU. He has served as the Director of the Institute of New Media and Communications, from 2009 to 2011. Prior to joining SNU, he was a Member of Technical Staff with AT&T Bell Laboratories, from 1991 to 1994, where he had worked on network management. He has been leading many industrial projects on 3G/4G/5G and the IoT connectivity supported by the Korean industry, and published more than 200 technical articles and holds more than 100 patents. He is a member of the National Academy of Engineering of Korea (NAEK) and the Whos Who Professional in Science and Engineering. He received the KICS Haedong Scholar Award in 2012. He has been serving as the Chief Information Officer (CIO) of SNU, the General Chair of IEEE Dynamic Spectrum Access and Networks (DySPAN) 2018, the General Chair of IEEE Wireless Communication and Networking Conference (WCNC) 2020, and the Director of Asia–Pacific region of IEEE ComSoc. He is also the President-Elect of the Korean Institute of Communications and Information Sciences (KICS), the TPC Chair of IEEE VTC-Spring 2014, and the General Chair of JCCI 2015. He is also the Co-EIC of the *Journal of Communications and Networks (JCN)* and an Editor of *IEEE Network Magazine*. He was on the editorial board of *Computer Networks (COMNET)* journal and IEEE TRANSACTIONS ON WIRELESS COMMUNICATIONS (TWireless).